J. Fluid Mech. (2011), *vol.* 679, *pp.* 32–57.
doi:10.1017/jfm.2011.109

Stokes drift dynamos

W. HERREMAN[1]† AND P. LESAFFRE[2]

[1]LIMSI, CNRS, 91403 Orsay CEDEX, France

[2]LERMA/LRA, CNRS/UMR8112, Ecole Normale Supérieure, 24, rue Lhomond, 75231 Paris, CEDEX 05, France

(Received 5 May 2010; revised 23 December 2010; accepted 2 March 2011; first published online 19 April 2011)

Fluid particles can have a mean motion in time, even when the Eulerian mean flow disappears everywhere in space. In the present article, we demonstrate that this phenomenon, known as the Stokes drift, plays an essential role in the problem of magnetic field generation by fluctuation flows (kinematic dynamo) at high Rm. At leading order, the dynamo is generated by the Stokes drift that acts as if it were a mean flow. This result is derived from a mean-field dynamo theory in terms of time averages, which reveals how classical expressions for alpha and beta tensors actually recombine into a single Stokes drift contribution. In a test case, we find fluctuation flows that have a G. O. Roberts flow as Stokes drift and this allows to confront our model to direct integration of the induction equation. We find an excellent quantitative agreement between the prediction of our model and the results of our simulations. We finally apply our Stokes drift model to prove that a broad class of inertial waves in rapidly rotating flows cannot drive a dynamo.

Key words: dynamo theory

1. Introduction

Dynamo theory has been developed over the last century to understand the origin of planetary and stellar magnetic fields. Some flows in electrically conducting fluid are capable of generating and sustaining a magnetic field without any external electromotive forces: we call these flows 'dynamos'. In the last two decades, numerical simulations have demonstrated that convectively driven turbulent flows are dynamos in many geometries (Glatzmaier & Roberts 1995; Busse 2002; Christensen 2008).

Before such simulations were possible, most of our understanding came from analytical calculations, such as those performed in the mean-field dynamo theory (Moffatt 1978; Krause & Rädler 1980). The idea of mean-field dynamo theory is that small-scale rapid magnetic fields fluctuations interact with velocity field fluctuations to promote the growth of a large-scale mean magnetic field. This analysis leads to the well-known alpha, beta or even higher order mean-field effects. For a recent review, see Brandenburg (2009).

Mean-field dynamo theories have been successful to describe dynamos in the diffusive (low-conductivity) limit. The best example of this success is the Karlsruhe dynamo (Stieglitz & Muller 2001). In this experiment, the growing magnetic fields have dominant large-scale structures which compare well with those calculated in a mean-field dynamo theory (Rädler *et al.* 2002). Yet, in most stars or planets,

† Email address for correspondence: wietze.herreman@limsi.fr

magnetic field advection strongly dominates over diffusion (high-conductivity limit). As large-scale magnetic fields are indeed observed in stellar or planetary magnetic fields, mean-field dynamo theories (Braginsky 1964; Moffatt 1978; Krause & Rädler 1980) have been proposed to model dynamos in this regime. Nevertheless, the validity of these formulae has always been under some scrutiny. Moreover, until a few years ago there were no critical tests that confronted this formalism to direct integrations of the induction equation. Recent years have witnessed such tests (Courvoisier, Hughes & Tobias 2006; Schrinner *et al.* 2007; Sur, Brandenburg & Subramanian 2008; Rädler & Brandenburg 2009) and each of them results in minor or even serious doubts about the validity of the mean-field theory in the high-conductivity limit: its improvement seems to be in order.

In our view, one basic feature of mean-field theory will always predestine its success: the choice of the average. We feel that a suitable average should at least capture the dominant part of the growing magnetic fields. When the chosen average is not motivated by actual features of the growing dynamos, mean-field formulae do not perform well (Courvoisier *et al.* 2006; Sur *et al.* 2008; Rädler & Brandenburg 2009). On the contrary, when an average reflects a dominant feature of the mean field, the mean-field formalism attains some success, e.g. axisymmetry worked quite well in Schrinner *et al.* (2007). This can be explained by the fact that mean-field dynamo calculations are rarely possible beyond the second order: few space scales next to the 'mean' scale are involved in the captured mechanism and this will not always be sufficient.

The problems related to unadapted spatial averages have motivated us to have a look back into mean-field dynamo theory without the use of spatial averaging. In the present article we reconsider magnetic-field generation by fluctuation flows with short correlation times in the high-conductivity limit. We find that mean-field dynamos can indeed be correctly captured in this limit if the 'mean' is defined as a time average and not as a spatial average. Incidentally, we also find that this leads to an appealing physical mechanism that is operational for a broad class of flows: at leading order, dynamo action by rapid fluctuation flows is controlled by the associated Stokes drift that acts on the mean field as if it were a mean flow. To the best of our knowledge, the Stokes drift (Stokes 1847) has never been considered in the dynamo context and we give here a brief feeling of how it comes into play. The Stokes drift captures the leading-order Lagrangian mean flow, i.e. the mean particle displacement induced by a fluctuation flow. In the zero-magnetic diffusivity limit, magnetic field lines are rigidly attached to fluid particles (Moffatt 1978). As these particles move on average through the Stokes drift, it is natural that time-averaged magnetic fields deform under the action of this drift. We demonstrate this idea rigorously in the frozen flux limit in § 2.1. Moreover, we also show how this leading-order role of the Stokes drift can be 'distilled' from a time-averaged Eulerian mean-field dynamo theory in the high-conductivity limit. This is demonstrated in §§ 2.2–2.3. We will explicitly show the link between our idea and the alpha and beta tensors, which have a longer history in mean-field dynamo theory (Moffatt 1978; Krause & Rädler 1980).

Serious testing is in order for any mean-field model that claims to capture dynamo action and such test is performed in § 3. We find fluctuation flows that have a G. O. Roberts flow (Roberts 1972) as Stokes drift. We compare our model to direct integrations of the induction equation. The fact that we do find Roberts-like dynamos and excellent quantitative agreement confirms the validity of our model.

We finally apply our model to the possible generation of magnetic field by inertial wave flows in rapidly rotating flows. Such waves are geophysically relevant as they

might be driven by precessional, librational or tidal deformations of celestial bodies (Malkus 1968; Aldridge & Toomre 1969; Kerswell 2002). Precessional dynamos have now been observed in several independent works (Tilgner 2005; Wu & Roberts 2008, 2009). Could inertial waves play a role in these dynamos? Up to now, this question has only been studied by Moffatt (1975) using a spatially averaged mean-field theory. Inertial waves actually ideally fit in our model. In § 4, we apply the Stokes drift model to study whether simple inertial waves in infinite space, plane fluid layers, cylinders, spheres and spheroids may drive kinematic dynamos. The final section concludes and discusses some perspectives.

2. Theoretical analysis

We consider the problem of magnetic field generation by rapid fluctuation flows in electrically conducting fluids. We note this flow $\boldsymbol{U}(\boldsymbol{x}, t)$ and the magnetic diffusivity of the fluid η. The problem is scaled in units

$$[\boldsymbol{U}] = U, \quad [\boldsymbol{x}] = R, \quad [t] = T, \tag{2.1}$$

where U and R are typical velocity and space scales, respectively. The time scale T is typically a period (for periodical flows) or a correlation time (for random flows). By 'fluctuation' flow, we mean that the flow has a disappearing time average at any place in space,

$$\overline{\boldsymbol{U}(\boldsymbol{x}, t)} = \boldsymbol{0}, \quad \forall \boldsymbol{x}, \quad \forall t. \tag{2.2}$$

The explicit definitions of these time averages depend on the flow and will be specified later. By 'rapid' we mean that the fluctuation flow varies on a time scale T which is very short compared to the advective time scale R/U and the diffusive time scale $R^2\eta$,

$$T \ll \frac{R}{U} \ll \frac{R^2}{\eta}. \tag{2.3}$$

In terms of dimensionless numbers, the above constraints imply

$$S = \frac{UT}{R} \ll 1, \quad Q = \frac{\eta T}{R^2} \ll 1, \quad Rm = \frac{UR}{\eta} = \frac{S}{Q} \gg 1. \tag{2.4}$$

In the case of random flows S is a Strouhal number. The hypothesis $S \ll 1$ is then a short correlation time assumption. Rm is a magnetic Reynolds number. Only two of these numbers are independent. We now consider the action of the flow on the magnetic field $\boldsymbol{b}(\boldsymbol{x}, t)$ by writing the following induction equation:

$$\partial_t \boldsymbol{b} = S\,\nabla \times (\boldsymbol{U} \times \boldsymbol{b}) + Q\,\Delta \boldsymbol{b}, \quad \nabla \cdot \boldsymbol{b} = 0, \tag{2.5}$$

where we use units (2.1). It is unusual to write this equation with its explicit dependence on two parameters rather than only Rm, but this is well funded for rapidly varying flows.

One advantage of the use of this rapid time scale in the induction equation is that (2.5) immediately displays a quite important feature of magnetic fields that may be generated by such 'rapid fluctuation flows'. It expresses clearly that magnetic fields cannot vary strongly on time scales much faster than the turnover time R/U of the flow, which is a well-known fact for even fast dynamos (Childress & Gilbert 1995). In a more formal way, we can imagine to write out asymptotical expansions for the

field $\boldsymbol{b}$ in terms of the small parameter S

$$\boldsymbol{b}(\boldsymbol{x},t)=\boldsymbol{b}^{(0)}(\boldsymbol{x},t)+S\,\boldsymbol{b}^{(1)}(\boldsymbol{x},t)+O(S^2). \tag{2.6}$$

Injecting these expansions in the induction equation, we find at zeroth order that

$$\partial_t\boldsymbol{b}^{(0)}(\boldsymbol{x},t)=0\Rightarrow\boldsymbol{b}^{(0)}=\overline{\boldsymbol{b}^{(0)}}(\boldsymbol{x}). \tag{2.7}$$

The dominant $O(1)$ part of the magnetic field may not vary on the short time scale of the flow. Consequently, it may only be a 'mean' field (constant on the short time scale). Time-dependent magnetic field 'fluctuations' can first appear at order $O(S)$. This implies that fluctuation dynamos, in the sense of magnetic fields that strongly vary on the short time scale T, are excluded in the asymptotical limit ($S\ll1$, $Q\ll1$).

The previous argument justifies a mean-field theory based on time averages, but this is however not transposable to an approach based on spatial averages. Nevertheless, the mean-field dynamo theory for general averages is quite well-established (Moffatt 1978; Krause & Rädler 1980) and known as the high-conductivity limit short correlation time approximation. As discussed in the Introduction, serious doubts currently exist about the validity of these mean-field approaches (Courvoisier *et al.* 2006; Rädler & Brandenburg 2009). We therefore reconsider the problem of mean-field dynamo action in the short correlation time limit using time averages only.

2.1. *Stokes drift and frozen flux limit*

It is instructive to consider the behaviour of time-averaged magnetic fields in the ideal magnetohydrodynamical or frozen flux limit, where magnetic diffusion is neglected,

$$Q,\,Rm^{-1}\to0. \tag{2.8}$$

The vocabulary 'frozen flux' finds its origin in the fact that magnetic field lines are rigidly attached to fluid particles or 'frozen' in the fluid. This can be translated in terms of the formal Cauchy solution that involves Lagrangian variables and coordinates. To express this solution, we consider particle trajectories $\boldsymbol{x}(\boldsymbol{a},t)$ that solve

$$\partial_t\,\boldsymbol{x}(\boldsymbol{a},t)=S\,\boldsymbol{U}\big(\boldsymbol{x}(\boldsymbol{a},t),t\big),\quad \boldsymbol{x}(\boldsymbol{a},0)=\boldsymbol{a}. \tag{2.9}$$

In integral form, we have

$$\boldsymbol{x}(\boldsymbol{a},t)=\boldsymbol{a}+S\int_0^t\boldsymbol{U}(\boldsymbol{x}(\boldsymbol{a},t'),t')\,\mathrm{d}t', \tag{2.10}$$

where we use units (2.1). The Lagrangian velocity and magnetic fields are defined as

$$\boldsymbol{U}^L(\boldsymbol{a},t)=\boldsymbol{U}\big(\boldsymbol{x}(\boldsymbol{a},t),t\big),\quad \boldsymbol{b}^L(\boldsymbol{a},t)=\boldsymbol{b}(\boldsymbol{x}(\boldsymbol{a},t),t). \tag{2.11}$$

If we now have some initial magnetic field $\boldsymbol{b}_0(\boldsymbol{a})$, the Cauchy solution gives the magnetic field at any time (see, for example, Molchanov, Ruzmaikin & Sokolov (1985)) in terms of the trajectories only

$$\boldsymbol{b}^L(\boldsymbol{a},t)=\boldsymbol{b}_0(\boldsymbol{a})\cdot\nabla_a\,\boldsymbol{x}(\boldsymbol{a},t). \tag{2.12}$$

Here, ∇_a is the del-operator that acts on initial positions $\boldsymbol{a}$. In practice, this formula is rarely useful, simply because particle trajectories are quite hard to determine. Let us look at the behaviour of time-averaged fields. We start from the previous formal solution and differentiate both sides over time:

$$\partial_t\boldsymbol{b}^L(\boldsymbol{a},t)=S\,\boldsymbol{b}_0(\boldsymbol{a})\cdot\nabla_a\,\boldsymbol{U}^L(\boldsymbol{a},t). \tag{2.13}$$

This is just the induction equation (2.5) in Lagrangian form, with an initial condition that has been specified and of course $Q=0$. We average this frozen flux solution over time using an operation

$$\overline{f}(s)=\int_s^{s+1} f(t)\,\mathrm{d}t \tag{2.14}$$

and suppose for now a periodical flow with unitary period, so that the flow is indeed a fluctuation flow. Applying this average or more precisely 'smoothing procedure' on (2.13), we get

$$\overline{\partial_t \boldsymbol{b}^L(\boldsymbol{a},t)}=S\,\boldsymbol{b}_0(\boldsymbol{a})\cdot\nabla_a\,\overline{\boldsymbol{U}^L(\boldsymbol{a},t)}. \tag{2.15}$$

The mean evolution of the magnetic field along Lagrangian particle trajectories is entirely controlled by the Lagrangian mean flow. In the present case of fluctuation flows, the Lagrangian mean flow is actually nothing else but the Stokes drift (Stokes 1847). We now obtain a practical leading-order formula for this drift. Whenever $S\ll 1$, fluid particles cannot drift too far apart within one averaging time

$$||\boldsymbol{x}(\boldsymbol{a},t)-\boldsymbol{x}(\boldsymbol{a},s)||\ll 1,\quad \forall t\in[s,s+1]. \tag{2.16}$$

We can then use a Taylor expansion for the Lagrangian mean flow $\overline{\boldsymbol{U}^L(\boldsymbol{a},t)}$ around a fixed position $\boldsymbol{x}(\boldsymbol{a},s)$ at all times $t\in[s,s+1]$

$$\overline{\boldsymbol{U}(\boldsymbol{x}(\boldsymbol{a},t),t)}=\underbrace{\overline{\boldsymbol{U}(\boldsymbol{x}(\boldsymbol{a},s),t)}}_{=0}+\underbrace{\overline{(\boldsymbol{x}(\boldsymbol{a},t)-\boldsymbol{x}(\boldsymbol{a},s))\cdot\nabla_x\boldsymbol{U}(\boldsymbol{x}(\boldsymbol{a},s),t)}}_{\text{Stokes drift}}+\cdots \tag{2.17}$$

The first term disappears because it is the Eulerian mean flow at fixed position $\boldsymbol{x}(\boldsymbol{a},s)$ (see (2.2)). The second term is the Stokes drift. Inspecting the formula, we understand that it is a net difference of velocity along particle trajectories that induces the mean particle transport captured in the Stokes drift. We substitute

$$\boldsymbol{x}(\boldsymbol{a},t)-\boldsymbol{x}(\boldsymbol{a},s)=S\int_s^t \boldsymbol{U}(\boldsymbol{x}(\boldsymbol{a},t'),t')\,\mathrm{d}t' \tag{2.18}$$

and use yet another Taylor expansion as in (2.17) to rewrite the Lagrangian flow in this integrandum. This leads to the leading-order formula for the Lagrangian mean flow or Stokes drift:

$$\overline{\boldsymbol{U}^L(\boldsymbol{a},t)}=S\,\boldsymbol{V}_{st}(\boldsymbol{x}(\boldsymbol{a},s),s)+O(S^2). \tag{2.19}$$

Here and further, we note $\boldsymbol{V}_{st}$ as the rescaled Stokes drift given by the following formula:

$$\boldsymbol{V}_{st}(\boldsymbol{x},s)=\overline{\left(\int_s^t \boldsymbol{U}(\boldsymbol{x},t')\,\mathrm{d}t'\right)\cdot\nabla\boldsymbol{U}(\boldsymbol{x},t)}. \tag{2.20}$$

This formula has an Eulerian character, but in (2.19) we do find a Lagrangian variable. Substituting this result back in the averaged evolution equation, we have

$$\overline{\partial_t \boldsymbol{b}^L}(\boldsymbol{a},s)=S^2\,\boldsymbol{b}_0(\boldsymbol{a})\cdot\nabla_a\left(\boldsymbol{V}_{st}^L(\boldsymbol{a},s)+O(S)\right). \tag{2.21}$$

At leading order, the mean evolution of the magnetic field along Lagrangian particle trajectories is controlled by the Stokes drift. We now go one step further by using

$$\overline{\partial_t \boldsymbol{b}^L(\boldsymbol{a},t)}=\partial_s\overline{\boldsymbol{b}^L(\boldsymbol{a},t)}(s), \tag{2.22}$$

which is exact for the average (2.14). This allows to write an evolution equation for the time 'smoothed' magnetic field. A similar Taylor expansion for the Lagrangian

mean magnetic field around position $\boldsymbol{x}(\boldsymbol{a}, s)$ leads to

$$\overline{\boldsymbol{b}(\boldsymbol{x}(\boldsymbol{a}, t), t)} = \overline{\boldsymbol{b}(\boldsymbol{x}(\boldsymbol{a}, s), t)} + \overline{(\boldsymbol{x}(\boldsymbol{a}, t) - \boldsymbol{x}(\boldsymbol{a}, s)) \cdot \nabla_x \boldsymbol{b}\big(\boldsymbol{x}(\boldsymbol{a}, s), t\big)} + \cdots$$
$$= \overline{\boldsymbol{b}}(\boldsymbol{x}(\boldsymbol{a}, s), s) + O(S). \tag{2.23}$$

We decide to keep the leading-order first term only that defines a smoothed magnetic field $\overline{\boldsymbol{b}}$ in Lagrangian form. Substituting this expression in the evolution equation, we find

$$\partial_s(\,\overline{\boldsymbol{b}}(\boldsymbol{x}(\boldsymbol{a}, s), s) + O(S)) = S^2\, \boldsymbol{b}_0(\boldsymbol{a}) \cdot \nabla_a (\boldsymbol{V}_{st}\big(\boldsymbol{x}(\boldsymbol{a}, s), s) + O(S)). \tag{2.24}$$

The S^2-prefactor of the right-hand side can be absorbed in a new slow time scale $\tau = S^2 s$. The previous equation then finally tells us that when magnetic diffusivity is neglected: at leading order, the time-averaged magnetic field evolves as if it is frozen into the Stokes drift $\boldsymbol{V}_{st}$ associated with the fluctuation flow $\boldsymbol{U}$. Dynamo action is formally excluded in this frozen flux limit, but still this result is a first argument in favour of our claim formulated in the Introduction.

2.2. *Eulerian mean-field dynamo theory: simple wave-like flow*

We now show that the leading-order role of Stokes drift can be 'distilled' from a time-averaged Eulerian mean-field dynamo theory in the low diffusivity, second order correlation approximation (SOCA) limit. This approach will also show the explicit link between our idea and the alpha and beta tensors that have a longer history in mean-field dynamo theory (Moffatt 1978; Krause & Rädler 1980). We first present Eulerian mean-field dynamo theory for the specific case of a simple wave-like incompressible flow which is the easiest to model

$$\boldsymbol{U}(\boldsymbol{x}, t) = \boldsymbol{u}(\boldsymbol{x})\, \mathrm{e}^{\mathrm{i}t} + \text{c.c.}, \quad \nabla \cdot \boldsymbol{u} = 0, \tag{2.25}$$

where c.c. stands for complex conjugated. The 2π-periodic flow is written in non-dimensional form $T = \omega^{-1}$, with ω being the dimensional rotation frequency and R being a wavelength. In this example we can use a time average

$$\overline{f} = \frac{1}{2\pi} \int_0^{2\pi} f \, \mathrm{d}t. \tag{2.26}$$

The time-averaged Eulerian flow disappears everywhere in space $\overline{\boldsymbol{U}(\boldsymbol{x}, t)} = \boldsymbol{0}$ so that is a fluctuation flow.

2.2.1. *Classical mean-field theory*

We propose magnetic field solutions of the form

$$\boldsymbol{b} = [\,\overline{\boldsymbol{b}}(\boldsymbol{x}) + \boldsymbol{b}'(\boldsymbol{x}, t)]\, \mathrm{e}^{\sigma t}, \tag{2.27}$$

where

$$||\overline{\boldsymbol{b}}|| = O(1), \quad ||\boldsymbol{b}'|| = O(S). \tag{2.28}$$

Note this is consistent with (2.7). Formula (2.27) explicitly states that exponentially growing solutions have both mean and fluctuating parts: this is motivated by the linearity of the induction problem (2.5). We set $\overline{\boldsymbol{b}'} = 0$ by definition. We now split (2.5) in mean and fluctuating parts using the time-average equation (2.26),

$$\sigma \overline{\boldsymbol{b}} = S\, \nabla \times (\overline{\boldsymbol{U} \times \boldsymbol{b}'}) + Q\, \Delta \overline{\boldsymbol{b}}, \tag{2.29a}$$
$$\partial_t \boldsymbol{b}' + \sigma \boldsymbol{b}' = S\, \nabla \times (\boldsymbol{U} \times \overline{\boldsymbol{b}}) + Q\, \Delta \boldsymbol{b}' + S\, \nabla \times \big[\boldsymbol{U} \times \boldsymbol{b}' - (\overline{\boldsymbol{U} \times \boldsymbol{b}'})\big]. \tag{2.29b}$$

If we start from a magnetic field with a dominant mean part $\overline{\boldsymbol{b}} = O(1)$, the fluctuation field will be forced by the term $S\,\boldsymbol{\nabla} \times (\boldsymbol{U} \times \overline{\boldsymbol{b}}) = O(S)$, so that it indeed is of smaller magnitude. If we then substitute this $\boldsymbol{b}'$ back in the mean-field equation (2.29), the term $S\,\boldsymbol{\nabla} \times (\overline{\boldsymbol{U} \times \boldsymbol{b}'}) = O(S^2)$. Balancing all terms in the mean-field equation, we have a scaling argument for the growth rate and the parameter Q

$$\sigma = O(S^2), \quad Q = O(S^2). \tag{2.30}$$

Most often it will be necessary that $Q \ll S^2$ to have growing magnetic fields. As a consequence of these scalings, a lot of terms can be safely neglected at lowest order in the fluctuation equation

$$\sigma\,\boldsymbol{b}' = O(S^3), \quad Q\Delta\boldsymbol{b}' = O(S^3), \quad S\,\boldsymbol{\nabla} \times [\boldsymbol{U} \times \boldsymbol{b}' - (\overline{\boldsymbol{U} \times \boldsymbol{b}'})] = O(S^2). \tag{2.31}$$

Since we do not suppose space scale separation between $\boldsymbol{b}'$ and $\overline{\boldsymbol{b}}$, the diffusive term $Q\Delta\boldsymbol{b}'$ may indeed be neglected (spatial averages have trouble in controlling the magnitude of this term). The leading-order fluctuation problem reduces to

$$\partial_t \boldsymbol{b}' = S\,\boldsymbol{\nabla} \times [(\boldsymbol{u}\,\mathrm{e}^{\mathrm{i}t} + \text{c.c.}) \times \overline{\boldsymbol{b}}] + O(S^2). \tag{2.32}$$

These reductions allow us to calculate the fluctuation field as a function of the general mean field. We time-integrate equation (2.32) and get

$$\boldsymbol{b}' = \boldsymbol{b}'(\boldsymbol{x}, t_0) + S[-i(\overline{\boldsymbol{b}} \cdot \boldsymbol{\nabla}\boldsymbol{u} - \boldsymbol{u} \cdot \boldsymbol{\nabla}\overline{\boldsymbol{b}})\,\mathrm{e}^{\mathrm{i}t} + \text{c.c.}] + O(S^2). \tag{2.33}$$

The second step is to substitute this expression back into the mean-field equation to get a closed equation for the mean field alone. The mean electromotive force (emf) $\boldsymbol{\zeta}$ is here found as

$$\boldsymbol{\zeta}_i = (S\,\overline{\boldsymbol{U} \times \boldsymbol{b}'})_i = \alpha_{il}\,\overline{b}_l + \beta_{ilk}\,\partial_l\,\overline{b}_k, \tag{2.34}$$

with

$$\alpha_{il}(\boldsymbol{x}) = \; 2S^2\,\mathrm{Im}\,(\epsilon_{ijk}\,u_j^*\,\partial_l\,u_k), \tag{2.35a}$$

$$\beta_{ilk}(\boldsymbol{x}) = -2S^2\,\mathrm{Im}\,(\epsilon_{ijk}\,u_j^*\,u_l). \tag{2.35b}$$

Here Im stands for imaginary part and the partial derivative $\partial_l \equiv \partial/\partial x_l$. The initial field is time-independent and with $\overline{\boldsymbol{U}} = 0$, it does not contribute to the mean emf.

Up to now, we followed a rather classic path for the derivation of the mean-field tensors. Since we did not spatially average, the alpha and beta tensors are spatially dependent second- and third-rank tensors. Then, what did we really gain? Indeed, to solve the mean-field problem,

$$\sigma\overline{\boldsymbol{b}} = \boldsymbol{\nabla} \times \boldsymbol{\zeta}(\boldsymbol{x}) + Q\,\Delta\overline{\boldsymbol{b}}, \tag{2.36}$$

is nearly as hard as to solve the initial dynamo problem (2.5). This is why spatial averaging together with the use of symmetry arguments (Moffatt 1978; Krause & Rädler 1980) has been so popular in mean-field dynamo theory: complicated alpha and beta tensors reduce to a small number of mean-field coefficients. However, we will now show that after some manipulation the mean-field problem (2.36) can take an insightful form.

2.2.2. *Exact reductions*

We first write out the alpha tensor using (i) the fact that summed indices can be renamed, (ii) the properties of the Levi-Civita tensor and (iii) the properties of the

imaginary part operator:

$$\begin{aligned}\alpha_{il} &= S^2\,\mathrm{Im}\,(\epsilon_{ijk}\,u_j^*\,\partial_l\,u_k + \epsilon_{ikj}\,u_k^*\,\partial_l\,u_j)\\ &= S^2\,\mathrm{Im}\,(\epsilon_{ijk}\,u_j^*\,\partial_l\,u_k + \epsilon_{ijk}\,u_k\,\partial_l\,u_j^*)\\ &= S^2\partial_l[\mathrm{Im}\,(\epsilon_{ijk}\,u_j^*\,u_k)].\end{aligned} \tag{2.37}$$

This means that we may rewrite the alpha contribution to the mean emf as

$$\boldsymbol{\alpha}\,\overline{\boldsymbol{b}} = (\overline{\boldsymbol{b}}\cdot\nabla)\,\boldsymbol{\xi}, \quad \boldsymbol{\xi} = S^2\,\mathrm{Im}\,(\boldsymbol{u}^*\times\boldsymbol{u}). \tag{2.38}$$

In the $\boldsymbol{\beta}$-tensor, many terms disappear immediately: (i) terms β_{ilk} are zero when $i=k$ due to the properties of the Levi-Civita tensor, (ii) terms β_{ilk} with all different indices, $i\neq l\neq k$, are also zero since the imaginary part of a norm is always zero, $\mathrm{Im}(|\,u_l\,|^2)=0$ for $l=x,\,y,\,z$. In the remaining terms, velocity field variables are always combined as components of the field $\boldsymbol{\xi}$. We noticed that they can further be reduced in an interesting way. As an example, we show this in detail for the x-part of the emf related to the β-term:

$$\begin{aligned}\beta_{xlk}\,\partial_l\,\overline{b}_k &= -\xi_x\,(\,\partial_y\,\overline{b}_y + \partial_z\,\overline{b}_z) + \xi_y\,\partial_x\,\overline{b}_y + \xi_z\,\partial_x\,\overline{b}_z\\ &= \xi_x\,\partial_x\,\overline{b}_x + \xi_y\,\partial_x\,\overline{b}_y + \xi_z\,\partial_x\,\overline{b}_z\\ &= \partial_x\,(\boldsymbol{\xi}\cdot\overline{\boldsymbol{b}}) - (\overline{b}_x\,\partial_x\,\xi_x + \overline{b}_y\,\partial_x\,\xi_y + \overline{b}_z\,\partial_x\,\xi_z).\end{aligned} \tag{2.39}$$

We used Gauss' law ($\nabla\cdot\overline{\boldsymbol{b}}=0$) and elementary differentiation rules. Note that only partial derivatives ∂_x appear in the final formula. Similar simplifications occur in the y and z components of the emf related to the β-term. We then get an expression as (2.39) but with the ∂_x replaced by ∂_y or ∂_z, respectively. Summing up both alpha and beta parts and recombining the terms, we can actually rewrite the emf in a much simpler form,

$$\boldsymbol{\zeta} = \big(\nabla\times\boldsymbol{\xi}\,\big)\times\overline{\boldsymbol{b}} + \nabla\big(\boldsymbol{\xi}\cdot\overline{\boldsymbol{b}}\big). \tag{2.40}$$

The second term is a pure gradient that contributes to the mean emf, but not to the mean-field generation: taking the curl of the emf in (2.36), the contribution of this gradient disappears identically. Only the first term will survive. More precisely, we find

$$\nabla\times\boldsymbol{\xi} = 2\,S^2\,\mathrm{Im}\,(\boldsymbol{u}\cdot\nabla\boldsymbol{u}^*). \tag{2.41}$$

This term acts on the mean magnetic field as if it were a mean flow. Let us now calculate the Stokes drift associated with the wave-like flow under study. Using a formula similar to (2.20) with an average (2.26), we get

$$\begin{aligned}\boldsymbol{V}_{st} &= \frac{1}{2\pi}\int_0^{2\pi}\left[\int_0^t(\boldsymbol{u}\,\mathrm{e}^{\mathrm{i}t} + \boldsymbol{u}^*\,\mathrm{e}^{-\mathrm{i}t})\,\mathrm{d}t'\right]\cdot\nabla(\boldsymbol{u}\,\mathrm{e}^{\mathrm{i}t} + \boldsymbol{u}^*\,\mathrm{e}^{-\mathrm{i}t})\,\mathrm{d}t\\ &= \frac{1}{2\pi}\int_0^{2\pi}(-i\,\boldsymbol{u}\,(\,\mathrm{e}^{\mathrm{i}t}-1) + i\,\boldsymbol{u}^*\,(\mathrm{e}^{-\mathrm{i}t}-1))\cdot\nabla(\boldsymbol{u}\,\mathrm{e}^{\mathrm{i}t} + \boldsymbol{u}^*\,\mathrm{e}^{-\mathrm{i}t})\,\mathrm{d}t\\ &= 2\,\mathrm{Im}\,(\boldsymbol{u}\cdot\nabla\boldsymbol{u}^*).\end{aligned} \tag{2.42}$$

We identify the first term as the Stokes drift contribution

$$\nabla\times\boldsymbol{\xi} = S^2\,\boldsymbol{V}_{st}. \tag{2.43}$$

Finally, by rescaling time

$$\tau = S^2\,t, \quad \sigma_\tau = \frac{\sigma}{S^2}, \tag{2.44}$$

we get the mean-field 'induction' equation

$$\sigma_\tau \overline{\boldsymbol{b}} = \boldsymbol{\nabla} \times (\boldsymbol{V}_{st} \times \overline{\boldsymbol{b}}) + \mathscr{R}^{-1} \Delta \overline{\boldsymbol{b}}, \quad \mathscr{R} = \frac{S^2}{Q} = \frac{U\frac{U}{\omega}}{\eta}. \tag{2.45}$$

This result confirms our claim of § 2.1: at leading order, the action of wave-like fluctuation flows on a mean magnetic field is controlled by the associated Stokes drift which acts as a mean flow. Since we do not average over space, the Stokes drift $\boldsymbol{V}_{st}$ may indeed be a dynamo. Also note how the new magnetic Reynolds number $\mathscr{R}$ is the single remaining parameter in the problem. This implies that for fixed flows but varying S and Q, the rescaled growth rate is a function of $\mathscr{R}$ only: $\sigma_\tau = f(\mathscr{R})$. Also note how the relevant space scale in $\mathscr{R}$ is no longer R but the gyration radius U/ω of fluid particles.

2.3. *Eulerian mean-field dynamo theory: extensions*

We extend the previous result to periodical and random incompressible flows. Technical details on the simplifications in the random flow case are gathered in Appendix A. All formulae can also be applied to compressible flows, as explained in Appendix B. The effect of a small mean flow can also be modelled easily, see Appendix C.

2.3.1. *Periodical flows*

The single wave case is immediately extended to general periodical flows

$$\boldsymbol{U}(\boldsymbol{x}, t) = S \sum_{j=1}^{\mathscr{J}} (\boldsymbol{u}_j(\boldsymbol{x})\, \mathrm{e}^{\mathrm{i}jt} + \text{ c.c.}). \tag{2.46}$$

If each wave has its own typical magnitude and wavelength, it is necessary that $S = \max(S_j) \ll 1$, with $S_j = U_j/\omega_j R_j$ to meet the conditions under which the model can be applied (see (2.4)). Each frequency component adds a contribution weighted by j^{-1} to a total Stokes drift:

$$\boldsymbol{V}_{st} = 2 \sum_{j=1}^{\mathscr{J}} \mathrm{Im}(\boldsymbol{u}_j \cdot \boldsymbol{\nabla} \boldsymbol{u}_j^*)/j. \tag{2.47}$$

As in the single wave case, the mean magnetic field satisfies an induction equation (2.45) in which only the Stokes drift controls the leading-order magnetic field evolution.

2.3.2. *Random flows*

We consider a random fluctuation flow that is a realisation of a stochastic process. We assume an ergodic and stationary process: time averages are equivalent to ensemble averages and are time-independent. The following correlation tensors and spectra are supposed to be known:

$$R_{ij}(\boldsymbol{x}, \Delta) = \overline{U_i(\boldsymbol{x}, t + \Delta)\, U_j(\boldsymbol{x}, t)} = \int_{-\infty}^{+\infty} \Phi_{ij}(\boldsymbol{x}, \omega)\, \mathrm{e}^{\mathrm{i}\omega\Delta}\, \mathrm{d}\omega, \tag{2.48a}$$

$$T_{ij}^k(\boldsymbol{x}, \Delta) = \overline{U_i(\boldsymbol{x}, t + \Delta)\, \partial_k U_j(\boldsymbol{x}, t)} = \int_{-\infty}^{+\infty} \Psi_{ij}^k(\boldsymbol{x}, \omega)\, \mathrm{e}^{\mathrm{i}\omega\Delta}\, \mathrm{d}\omega. \tag{2.48b}$$

Here, we use the correlation time as our typical time scale T. Namely, both R_{ij} and T_{ij}^k are quickly decaying functions with Δ.

We first perform the same operations, as in the classical analysis for the SOCA high-conductivity limit, for random flows with short correlation times (Krause & Rädler 1980). The mean emf has the same structure as before (2.34), with

$$\alpha_{il} = S^2 \int_0^{+\infty} \epsilon_{ijk}\, T^l_{jk}(\boldsymbol{x}, \Delta)\, \mathrm{d}\Delta, \tag{2.49a}$$

$$\beta_{ilk} = -S^2 \int_0^{+\infty} \epsilon_{ijk}\, R_{jl}(\boldsymbol{x}, \Delta)\, \mathrm{d}\Delta. \tag{2.49b}$$

See Appendix A for the details of the derivation. The S^2-prefactor is absent in a classical formula (Krause & Rädler 1980), but this is merely a consequence of our use of the short correlation time as a time scale in the induction equation.

We transform these formulae (see Appendix A) into a simplified mean emf of the form

$$\boldsymbol{\zeta} = (\boldsymbol{\nabla} \times \boldsymbol{\xi}) \times \overline{\boldsymbol{b}} + \boldsymbol{\nabla}(\boldsymbol{\xi} \cdot \overline{\boldsymbol{b}}) + \boldsymbol{\alpha}^R \overline{\boldsymbol{b}} + \boldsymbol{\beta}^R \boldsymbol{\nabla} \overline{\boldsymbol{b}}, \tag{2.50}$$

with

$$\xi_i = S^2 \int_0^{+\infty} \mathrm{Im}\left(\frac{\epsilon_{ikj}\, \Phi_{jk}(\boldsymbol{x}, \omega)}{\omega} \right) \mathrm{d}\omega \tag{2.51}$$

and

$$\alpha^{\mathrm{R}}_{il} = S^2\, \pi\, \epsilon_{ijk}\, \Psi^l_{jk}(\boldsymbol{x}, 0), \tag{2.52a}$$

$$\beta^{\mathrm{R}}_{ilk} = -S^2\, \pi\, \epsilon_{ijk}\, \Phi_{jl}(\boldsymbol{x}, 0). \tag{2.52b}$$

The mean magnetic field satisfies

$$\sigma_\tau \overline{\boldsymbol{b}} = \boldsymbol{\nabla} \times (\boldsymbol{V}_{st} \times \overline{\boldsymbol{b}}) + \boldsymbol{\nabla} \times (\widetilde{\boldsymbol{\alpha}} \overline{\boldsymbol{b}} + \widetilde{\boldsymbol{\beta}}\, \boldsymbol{\nabla} \overline{\boldsymbol{b}}) + \mathscr{R}^{-1}\, \Delta \overline{\boldsymbol{b}}, \tag{2.53}$$

with

$$(\boldsymbol{V}_{st})_i = \int_0^{+\infty} 2\, \mathrm{Im}\left(\frac{\Psi^j_{ji}(\boldsymbol{x}, \omega)}{\omega} \right) \mathrm{d}\omega, \tag{2.54}$$

and $\widetilde{\boldsymbol{\alpha}} = \boldsymbol{\alpha}^{\mathrm{R}}/S^2$ and $\widetilde{\boldsymbol{\beta}} = \boldsymbol{\beta}^{\mathrm{R}}/S^2$. The Stokes drift acts as a mean flow on the mean magnetic field, but supplementary terms related to the zero-frequency spectra do arise. In the magnetic Reynolds number $\mathscr{R} = U^2 T/\eta$, the typical distance over which particles move UT, appears as typical length scale. Since $\mathscr{R}$ is the only remaining parameter, we also have $\sigma_\tau = f(\mathscr{R})$ as before. Whenever the zero-frequency spectra disappear,

$$\Phi_{jl}(\boldsymbol{x}, 0) = 0, \quad \Psi^l_{jk}(\boldsymbol{x}, 0) = 0,\ \forall \boldsymbol{x} \Rightarrow \widetilde{\boldsymbol{\alpha}} = 0,\ \widetilde{\boldsymbol{\beta}} = 0, \tag{2.55}$$

the evolution of the mean magnetic field is then uniquely controlled by the Stokes drift. This case will be tested in what follows. If on the contrary the spectrum is real

$$\mathrm{Im}(\Phi_{jk}(\boldsymbol{x}, \omega)) = 0,\ \forall (\boldsymbol{x}, \omega) \Rightarrow \boldsymbol{\xi} = 0,\ \boldsymbol{V}_{st} = 0, \tag{2.56}$$

then only the zero-frequency spectra can affect the mean magnetic field. This case will not be tested hereafter. Note that zero-frequency terms did not appear in the Lagrangian argument of § 2.1. This part of the spectrum actually allows fluid particles to spread out over unbounded distances (Moffatt 1978) so that hypothesis (2.16) needs to be modified.

2.4. *Further discussion*

2.4.1. *Is the Stokes drift a 'magnetic pumping term'?*

Mean-field terms that act as flows on the mean magnetic field, so-called 'magnetic pumping' terms, often arise in classical mean-field dynamo theory. They derive from the antisymmetric part of the alpha tensor $\boldsymbol{\alpha}_a = (\boldsymbol{\alpha} - \boldsymbol{\alpha}^T)/2$. Interestingly, we find (no zero-frequency spectrum case) that

$$\boldsymbol{\alpha}_a \overline{\boldsymbol{b}} = \frac{S^2}{2} \boldsymbol{V}_{st} \times \overline{\boldsymbol{b}}. \tag{2.57}$$

Only half of the Stokes drift term finds its origin in the antisymmetric part of the alpha tensor. The second half follows from the combination of the symmetric part of the alpha tensor $\boldsymbol{\alpha}_s = (\boldsymbol{\alpha} + \boldsymbol{\alpha}^T)/2$ and the beta terms:

$$\boldsymbol{\alpha}_s \overline{\boldsymbol{b}} + \boldsymbol{\beta} \nabla \overline{\boldsymbol{b}} = \frac{S^2}{2} \boldsymbol{V}_{st} \times \overline{\boldsymbol{b}} + \nabla(\boldsymbol{\xi} \cdot \overline{\boldsymbol{b}}). \tag{2.58}$$

It is also here that the gradient term is produced. One may not interpret the Stokes drift as a classical magnetic pumping term that derives from the alpha tensor alone.

2.4.2. *Scales and non-dimensional numbers*

The result $\sigma_\tau = f(\mathscr{R})$ that the rescaled rate growth is a function of $\mathscr{R} = S^2/Q$ only, for fixed flows but arbitrary S and Q, is a mere consequence of the used approximations (short correlation time and low diffusivity limit). Still this is very rarely spelled out by most of the mean models in this limit. For this reason, it is instructive to show explicitly how this translates if other (more commonly used) scales are used to scale time in the induction equation:

$$\left.\begin{aligned} \text{correlation time scale:} \quad & [t] = T \rightarrow \sigma = S^2 f(\mathscr{R}), \\ \text{advective time scale:} \quad & [t] = \frac{R}{U} \rightarrow \sigma' = S f(\mathscr{R}), \\ \text{diffusive time scale:} \quad & [t] = \frac{R^2}{\eta} \rightarrow \sigma'' = \mathscr{R} f(\mathscr{R}). \end{aligned}\right\} \tag{2.59}$$

We also note that the magnetic Reynolds number $\mathscr{R} = S^2/Q = S\,Rm$ can range in large intervals, even when both S and Q are very small and Rm is very high. For the consistency of the analysis (namely, for the ordering of the terms in (2.30)), it is necessary that $S^2 > Q$ or $\mathscr{R} > 1$ (alternatively, $Rm > S^{-1}$).

2.4.3. *Quick link with classical mean-field result*

Through the analysis, we found alpha and beta tensors which are strictly the same as those found by previous authors (Krause & Rädler 1980) modulo our use of the rapid correlation time T time scale. Clearly, upon the same assumptions (isotropy and large-scale average) we will find the same result, but where do these terms hide in the present formalism? We notice that it is precisely the isotropic part (one third part of the trace) of $\widetilde{\boldsymbol{\alpha}}$ which links alpha to helicity:

$$\alpha_{class} = \frac{1}{3}\widetilde{\alpha}_{ii} = \frac{1}{3}\,\pi\,\epsilon_{ijk}\,\Psi^i_{jk}(\boldsymbol{x}, 0) = -\frac{1}{3}\int_0^{+\infty} \overline{\boldsymbol{U}(\boldsymbol{x}, t+\Delta)\cdot(\nabla \times \boldsymbol{U}(\boldsymbol{x}, t))}\,\mathrm{d}\Delta. \tag{2.60}$$

Through supplementary averaging over space, we get the classical result which relates the alpha effect to helicity. In a similar way one can isolate a local isotropic turbulent

diffusivity $\pi\ \Phi_{jj}(\boldsymbol{x}, 0)/3$ from the tensor $\widetilde{\boldsymbol{\beta}}$. The Stokes drift terms disappears upon supplementary spatial $\langle\cdot\rangle$ averaging as $\langle\boldsymbol{\nabla}\times\boldsymbol{\xi}\rangle=\boldsymbol{0}$. In our model, it is exactly the $\widetilde{\boldsymbol{\alpha}}$ and $\widetilde{\boldsymbol{\beta}}$ terms that contain the classical results of mean-field dynamo theory in the high-conductivity limit short correlation time approximation.

2.4.4. *Delta-correlated flows*

The particular case of delta-correlated flows has attracted quite some attention in dynamo theory (Moffatt 1978; Krause & Rädler 1980; Molchanov *et al.* 1985), as it allows calculations of alpha and beta tensors. In that case, the correlation time scale can no longer be used to non-dimensionalise the induction equation ($T=0$) and the infinite root mean square (r.m.s.) velocity precludes its use as a typical velocity scale ($U\to\infty$). However, we can realise a delta-correlated flow as a proper limit of random flows with finite T and U.

As discussed in the previous section our result can be rearranged in diffusive units $[t]=R^2/\eta$ to find the third equation of (2.59). In explicit form, we have $\sigma''=(U^2T/\eta)\,f(U^2T/\eta)$. Provided that the delta-correlated flow appears as a limit in which an effective diffusivity scale η_δ exists,

$$\lim_{U^{-1},T\to 0} \quad U^2T=\eta_\delta, \tag{2.61}$$

we can apply our model. However, since delta-correlated flows have a real spectrum $\mathscr{F}_\omega(\delta(\Delta))=1$, the Stokes drift terms will always vanish for them (see (2.54)). Only the contributions of $\widetilde{\boldsymbol{\alpha}}$ and $\widetilde{\boldsymbol{\beta}}$ are captured in delta-correlated models.

3. Test case: the G. O. Roberts Stokes drift dynamo

The previous sections have documented our claim about the role of the Stokes drift. For a large variety of fluctuation flows, we can reduce the complexity of the kinematic dynamo problem to that of solving another induction equation with the stationary Stokes drift flow. In this section, we confront our model directly to the induction equation. The idea of our test is to compare growth rates and spatial structures of the magnetic fields found by solving:

(i) the original induction equation (2.5) with a fluctuation flow $\boldsymbol{U}$;

(ii) the mean-field 'induction equation' (2.45) with associated Stokes drift $\boldsymbol{V}_{st}$.

Our theory predicts that both should yield results that are quantitatively similar up to order $O(S^2)$. Ideally, we wish to test our results on a flow which has a Stokes drift that acts as a dynamo. We will hence design our flow such that its associated Stokes drift will be a well-studied dynamo flow.

3.1. *Fluctuation flows with a G. O. Roberts-like Stokes drift*

The fluctuation flow we use for our tests is defined as

$$\boldsymbol{U}(x, y, t)=(\partial_y\Lambda\,\hat{\boldsymbol{x}}-\partial_x\Lambda\,\hat{\boldsymbol{y}}+\Lambda\,\hat{\boldsymbol{z}})\,f(t)+\text{c.c.}, \tag{3.1}$$

with

$$\begin{cases}\rho^2=1+\cos(x+y)+C, & C\geqslant 0\\ \chi\ \ =-\cos(x-y)\end{cases}, \qquad \Lambda=\rho(x, y)\,\mathrm{e}^{\mathrm{i}\,\chi(x,y)}, \tag{3.2}$$

and

$$\text{single wave:} \quad f(t) = \mathrm{e}^{\mathrm{i}t}, \tag{3.3a}$$

$$\text{periodical:} \quad f(t) = \sum_{j=1}^{50} A\, j^{-p}\, \mathrm{e}^{\mathrm{i}\phi_j}\, \mathrm{e}^{\mathrm{i}jt}, \tag{3.3b}$$

$$\text{random:} \quad f(t) = \int_0^{+\infty} A\, \frac{\omega^p}{1+\omega^{2p}}\, \mathrm{e}^{\mathrm{i}\phi(\omega)}\, \mathrm{e}^{\mathrm{i}\omega t}\, \mathrm{d}\omega. \tag{3.3c}$$

It will be studied in a periodical fluid domain $x, y \in (0, 2\pi)$. The exponent $p > 0$ in both random and periodical cases allows to modify the frequency content of $f(t)$ in a simple way. The phase noises ϕ_j and $\phi(\omega)$ are uniformly distributed $U(0, 2\pi)$ random phases. The parameter A is a normalisation factor that sets the r.m.s. value of $f(t)$ to unity $\overline{|f|^2} = 1$. All the previous fluctuation flows have their Stokes drift in the form of a G. O. Roberts flow:

$$\boldsymbol{V}_{st} = F\, \left(\partial_y \Gamma\, \hat{\boldsymbol{x}} - \partial_x \Gamma\, \hat{\boldsymbol{y}} + 2\Gamma\, \hat{\boldsymbol{z}}\right), \tag{3.4}$$

with

$$\Gamma = (\partial_x \rho^2)(\partial_y \chi) - (\partial_y \rho^2)(\partial_x \chi) = -\cos 2x + \cos 2y \tag{3.5}$$

and

$$\text{single wave:} \quad F = 1, \tag{3.6a}$$

$$\text{periodical:} \quad F = A^2 \sum_{j=1}^{50} j^{-(1+2p)} \leqslant 1, \tag{3.6b}$$

$$\text{random:} \quad F = A^2 \int_0^{+\infty} \frac{1}{\omega} \left(\frac{\omega^p}{1+\omega^{2p}}\right)^2 \mathrm{d}\omega. \tag{3.6c}$$

Exactly two periodicity cells of the Roberts flow fit in the computational box $x, y \in (0, 2\pi)$. The Stokes drift does not depend on the value of C nor the realization of the phase noises ϕ_j and $\phi(\omega)$. We always have $\tilde{\alpha} = \tilde{\beta} = 0$ for positive p in the case of random flows. With a Roberts-like Stokes drift, we really know what to expect form our model: a well-known dynamo that operates in large spans of the magnetic Reynolds number, here $\mathscr{R}$, see, for example Roberts (1972), Soward (1987) and Plunian and Rädler (2002) for published values for the growth rates and spatial structures of the dynamo.

Let us have a look at some characteristics of the fluctuation flow before performing the test. In figure 1, we show the spatial profile of the 'stream function' $\Lambda(x, y)$ in the plane using a grey-scale code. Notice how the flow is strongly modified by varying from $C = 0$ to $C = 5$. Also note the significant increase in the magnitude of the flow for $C = 5$.

In figure 2 we show the G. O. Roberts stream function $\Gamma(x, y)$ together with some Lagrangian particle paths projected in the x–y plane. These trajectories were numerically integrated from (2.9) for the simple wave case with $f(t) = \mathrm{e}^{\mathrm{i}t}$ and $S = 0.1$. The particles combine quick oscillations with a mean drift that closely follows the G. O. Roberts streamlines, as expected from the Stokes drift formula.

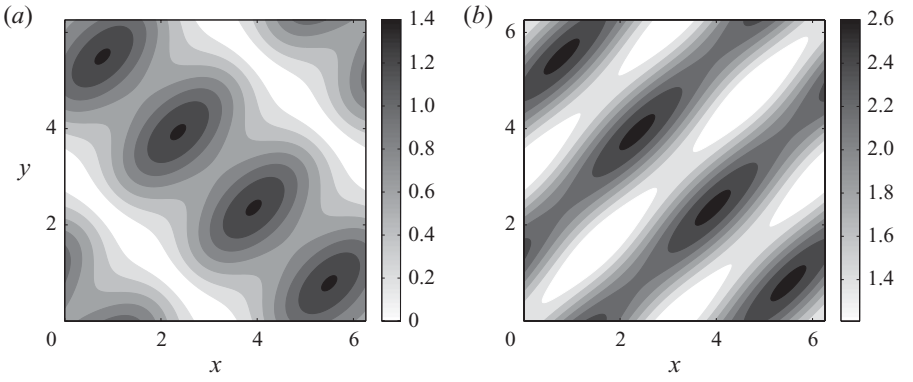

FIGURE 1. Visualisation of the real part of $\Lambda(x, y) = \rho(x, y)\, e^{i\chi(x,y)}$ defined by (3.2) for different values of the constant C. (*a*) $C = 0$, (*b*) $C = 5$.

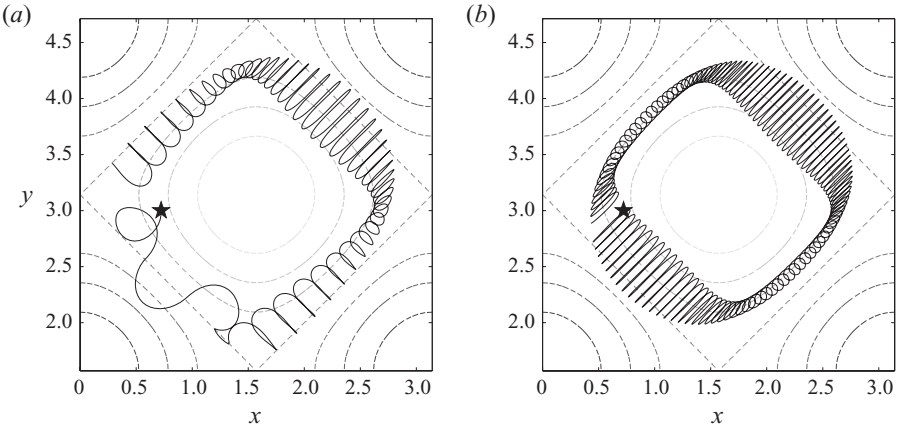

FIGURE 2. The Lagrangian particle trajectories for wave-like flows (3.1)–(3.2), with $f(t) = e^{it}$ follow the Roberts flow streamlines (3.5) on average. The star denotes the initial particle position. $S = 0.1$, (*a*) $C = 0$, (*b*) $C = 5$.

Figure 3 displays a similar figure but using three different periodical signals, with different exponents $p = 1, 1/2, 1/3$. With decreasing p, a particle drifts less far in the same amount of time, but it always closely follows the G. O. Roberts streamlines. This illustrates the formula for F: the magnitude of the Stokes drift decreases together with the exponent p for similarly normalised flows.

3.2. *Numerical method for the dynamo problem*

We used a pseudo-spectral solver that time steps the kinematic dynamo problems with (i) the fluctuation flow and (ii) the Stokes drift independently. For the G. O. Roberts flow, we also programmed a purely spectral solver that allowed us to test the pseudo-spectral code. Magnetic field solutions are decomposed on a Fourier basis,

$$\boldsymbol{b} = \sum_{k_x=-N/2+1}^{N/2} \sum_{k_y=-N/2+1}^{N/2} \left(\tilde{b}_x(\boldsymbol{k}),\, \tilde{b}_y(\boldsymbol{k}),\, \tilde{b}_z(\boldsymbol{k})\right) e^{i(k_x x + k_y y)}\, e^{ik_z z}. \tag{3.7}$$

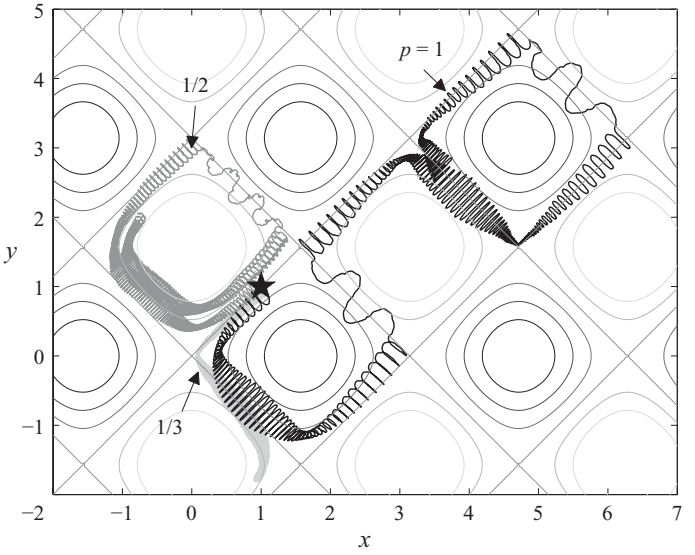

FIGURE 3. The Lagrangian particle trajectories over 200 periods of a general periodic flow (3.3*b*) with different exponents p. Fluid particles drift along the Roberts flow streamlines over distances that decrease together with the exponent p.

Since all flows are z-independent, modes with different vertical structure are decoupled: k_z is a vertical wavenumber that can be fixed *a priori* in both problems (i) and (ii). We solve the x and y projections of the induction equation, in which only b_x and b_y appear. With these fields and Gauss' law, we can reconstruct b_z *a posteriori*. We use a semi-implicit time-stepper, where the diffusive part is treated using the backward Euler scheme. The interaction with the flow is modelled with a second-order explicit Adams–Bashforth scheme. The code is dealiased using the 2/3-rule.

Each time, the most unstable mode that is generated from the initial state $(b_x, b_y) = (1, -i) \times 10^{-3} N^{-2}$ is followed. Growth rates σ are derived from exponential fits of the square root of the magnetic energy in the case (i) of fluctuation flows. They are then rescaled on the slow τ-time scale, $\sigma_\tau = \sigma / S^2$. In the second case (ii) we solve the mean induction equation with the G. O. Roberts-like Stokes drift. These theoretical growth rates are noted as $\sigma_{th} = F\, \sigma_{GO}(\mathscr{R}F)$. The values $\sigma_{GO}(\mathscr{R})$ correspond to the case with $F = 1$ and are through some rescaling (of space), identical to the growth rates reported in the literature (Roberts 1972; Soward 1987; Plunian & Rädler 2002).

Our theory requires small parameters S and Q and it is necessary to test the resolution that is needed to obtain results that are precise enough. In a small convergence test for the parameters $S = 0.1$, $Q = 10^{-3}$ and $k_z = 1$, we measured the growth rates $\sigma_\tau = 0.6307$ for $N = 32$, $\sigma_\tau = 0.6614$ for $N = 64$, $\sigma_\tau = 0.6576$ for $N = 128$ and $\sigma_\tau = 0.6572$ for $N = 256$. The growth rate σ_τ is converged up to the third digit for $N = 128$. This resolution will be sufficient in the following calculations.

3.3. *Results*

3.3.1. *Single wave flows*

We start the test with the single wave case and look for eigenmodes with vertical wavenumber $k_z = 1$. The fluctuation flows have $C = 0$ and 5. We first varied $S \in [0.04, 0.14]$ and fixed $Q = 10^{-3}$.

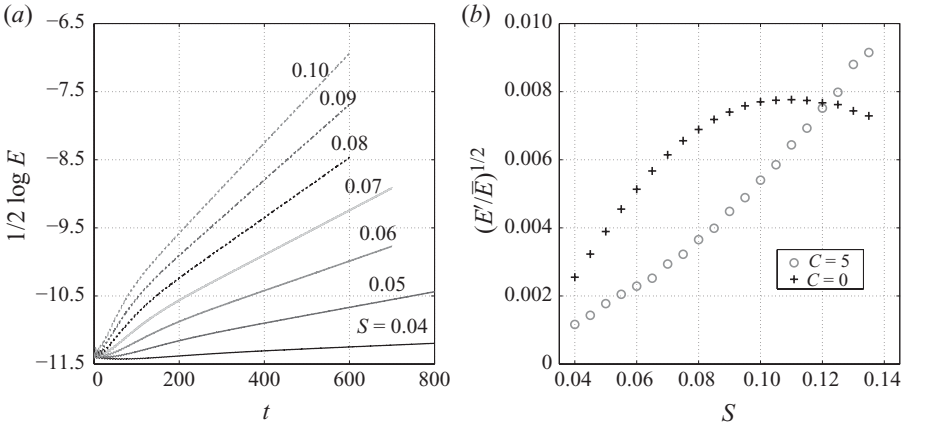

FIGURE 4. (*a*) Temporal growth of energy $E = \int\int (b_x^2 + b_y^2)\,\mathrm{d}x\,\mathrm{d}y$ for different values of S for $C = 0$. (*b*) The fluctuation to mean ratio of $E^{1/2}$ as a function of S for different C. $Q = 10^{-3}$, $k_z = 1$, $f(t) = \mathrm{e}^{\mathrm{i}t}$.

In figure 4(*a*) we plotted typical time series for the energy measure $E = \int\int (b_x^2 + b_y^2)\,\mathrm{d}x\,\mathrm{d}y$. An exponential growth is clearly established after some short transient. We only see small fluctuations in the time series. Rapidly varying magnetic fields are indeed much smaller in magnitude than the slowly varying part. This is more precisely measured in figure 4(*b*). The part of the magnetic field that fluctuates is typically over 100 times lower than the stationary mean component, which validates the assumption (2.28) of the mean-field modelling.

The growth rate σ is measured for all different S through linear fitting of $1/2 \log E \sim \sigma t$. In figure 5(*a*), we compare the rescaled growth rate $\sigma_\tau = \sigma/S^2$ to the theoretical growth rates $\sigma_{th} = \sigma_{GO}(\mathscr{R})$ (continuous line) as a function of the new magnetic Reynolds number $\mathscr{R} = S^2/Q$. The agreement is very good, independent of the choices of $C = 0$ or $C = 5$.

For larger S, the error increases, most probably because we are leaving the interval $S \ll 1$. This is better specified in figure 5(*b*), which plots the absolute error on the growth rate $\Delta\sigma = \sigma - S^2\sigma_{th}$. Apparently this error scales as $\Delta\sigma \sim S^6$ for large S, which suggests that our second-order mean-field model (in S) is correct up to sixth-order corrections for the flow under study. The plot also reveals some error for the lower S regime that was not visible in figure 5(*a*). These cases correspond to low $\mathscr{R} \simeq 1$, outside the non-diffusive regime of our theory.

The comparison between theory and numerical results is further continued in table 1, which shows some numerical values of the growth rates and the relative error $Er = |\sigma_{th} - \sigma_\tau|/\sigma_{th}$. There is an excellent agreement everywhere.

Let us now look at the spatial structure of the eigenmodes. In figure 6, we plotted the spatial structure of the mean magnetic energy $|\bar{\boldsymbol{b}}|^2$ of the unstable mode for the G. O. Roberts flow and from direct integrations with the wave-like flow in the cases $C = 0$ and $C = 5$. The fields of the Roberts dynamo are very similar to those of the $C = 0$ case which confirms that the Stokes drift really plays a crucial role.

The difference is more important for the case $C = 5$. Only half of the strong field zones is present and field lines prefer to elongate along the (1, 1)-direction in the

S	$\mathscr{R}$	σ_{th}	C	σ_τ	$Er\,(\%)$	C	σ_τ	$Er\,(\%)$
0.04	1.6	0.162	0	0.168	3.7	5	0.174	7.4
0.05	2.5	0.459	–	0.460	0.2	–	0.464	1.1
0.06	3.6	0.603	–	0.603	0.0	–	0.605	0.3
0.07	4.9	0.667	–	0.668	0.2	–	0.670	0.4
0.08	6.4	0.685	–	0.689	0.6	–	0.694	1.3
0.09	8.1	0.676	–	0.682	0.9	–	0.693	2.5
0.10	10	0.648	–	0.658	1.5	–	0.679	4.8

TABLE 1. Growth rate measurements and comparison with theoretical estimates for $f(t)=\mathrm{e}^{\mathrm{i}t}$, with $C=0,5$ and $Q=10^{-3}$. The mean-field theory is often accurate up to a few per cent in the relative measure $\Delta=|\sigma_{th}-\sigma_\tau|/\sigma_{th}$.

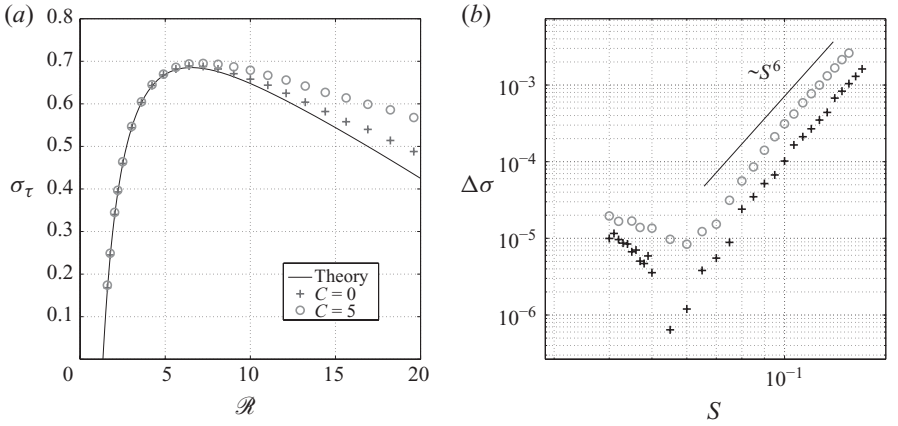

FIGURE 5. (a) Comparison of growth rate measures σ_τ for different $C=0,5$ to theoretical values as a function of magnetic Reynolds number $\mathscr{R}$. (b) Absolute growth rate difference $\Delta\sigma=\sigma-S^2\sigma_{th}$ as a function of S. $Q=10^{-3}$, $k_z=1$, $f(t)=\mathrm{e}^{\mathrm{i}t}$.

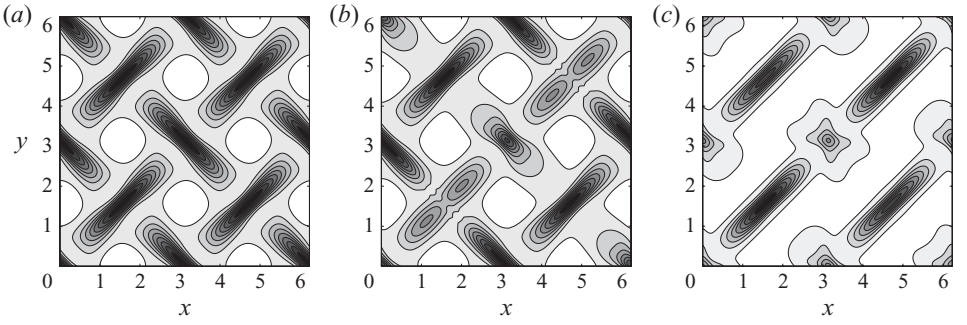

FIGURE 6. Comparison of mean magnetic energy $|\overline{\boldsymbol{b}}|^2$ of the dynamos excited by (a) the theoretical Roberts flow $\mathscr{U}$, (b) the fluctuation flow $\boldsymbol{U}$ with $C=0$, (c) the fluctuation flow $\boldsymbol{U}$ with $C=5$. Parameters are fixed as $Q=10^{-3}$, $k_z=1$, $S=0.1$, $\mathscr{R}=10$ and $f(t)=\mathrm{e}^{\mathrm{i}t}$.

x–y plane. This is mainly due to the chosen normalisation. Since flow speeds are significantly higher for the case $C=5$, than in the case $C=0$ (see figure 1), we leave the asymptotic regime of small S more early in the case $C=5$ than with $C=0$.

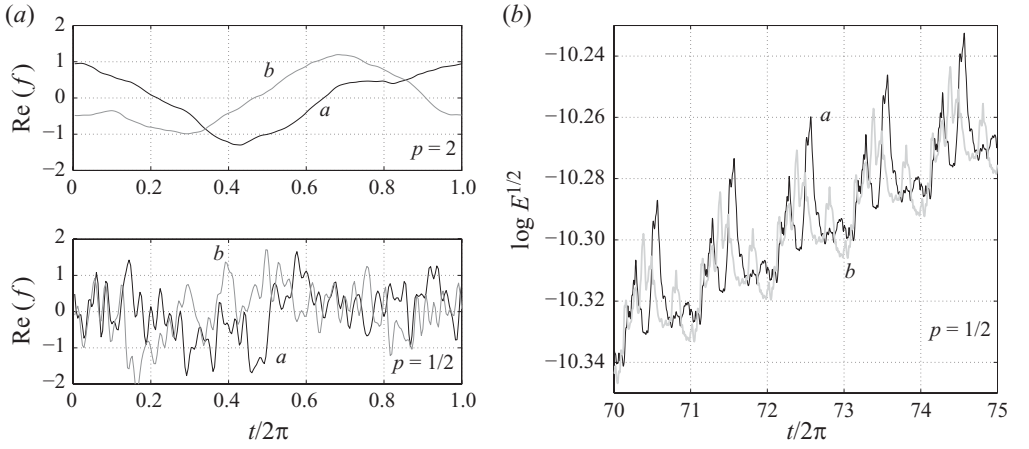

FIGURE 7. (*a*) Comparison of realizations of multifrequency signals $f(t)$ over one period according to (3.3*b*), for different exponents p and for different phase-noise realizations ϕ_j. (*b*) Zoom on temporal growth of energy $E = \int\int (b_x^2 + b_y^2)\,\mathrm{d}x\,\mathrm{d}y$ for exponent $p = 1/2$ using signals a and b for $f(t)$.

3.3.2. *Periodical flows*

We now perform some tests with periodical signals $f(t)$ using different exponents $p = 3, 2, 1, 1/2, 1/3$. For each value of p, we compare two different signals, referred to as a and b, that have been constructed using different realizations of the random phase noise ϕ_j.

Figure 7(*a*) shows the effect of the exponent $p = 2, 1/2$ on the signals $\mathrm{Re}(f)$ used in the calculations below. For high p, only low frequencies are relevant and the signal is mostly sinusoidal. For low p, the signal requires a noisy character. Also note how signals a and b are clearly different.

We now fix the parameters to $S = 0.1$, $Q = 10^{-3}$, $k_z = 1$, $C = 0$ and solve the kinematic dynamo problem (i) with the periodical fluctuation flow. An example of the growth of the magnetic energy is shown in figure 7(*b*). Within one period, fluctuations clearly depend on the precise realization of the function $f(t)$, but the mean growth over longer times is clearly independent of the realization of the phase noise, as predicted by the theory.

The growth rates are measured as before. In table 2, we compare the rescaled growth rates σ_τ to the theoretical growth rates $\sigma_{th} = F\,\sigma_{GO}(\mathscr{R}F)$. Here $\sigma_{GO}(\mathscr{R})$. The relative error Δ does not exceed a few per cent so that we can say that there is an excellent agreement.

3.3.3. *Random fluctuation flows*

We now test random functions $f(t)$. Let us first add some practical notes about the procedure that was used to construct such signals. Given the time step of the kinematic dynamo problem and the total integration period, we find the total number of time steps. This also defines the total number of random phases $\phi(\omega) \in U(0, 2\pi)$. The phase factors $\exp(i\phi(\omega))$ are then multiplied with the specified spectrum and the signal $f(t)$ is finally obtained by an inverse Fourier transform. We study spectra with exponents $p = 3, 2, 1, 1/2, 1/3$ and for each value of p, we compare two different realisations referred to as a and b.

Periodic	p	F	σ_{th}	σ_τ	Er (%)	Random	p	F	σ_{th}	σ_τ	Er (%)
a	3	0.991	0.644	0.653	1.5	a	3	0.954	0.626	0.641	2.4
b	–	–	–	0.653	1.5	b	–	–	–	0.649	3.7
a	2	0.958	0.627	0.636	1.4	a	2	0.900	0.598	0.600	0.3
b	–	–	–	0.636	1.4	b	–	–	–	0.583	2.5
a	1	0.740	0.504	0.507	0.5	a	1	0.653	0.447	0.428	4.3
b	–	–	–	0.506	0.3	b	–	–	–	0.439	1.8
a	1/2	0.361	0.218	0.218	0.0	a	1/2	0.326	0.186	0.183	1.6
b	–	–	–	0.217	0.5	b	–	–	–	0.197	5.9
a	1/3	0.233	0.098	0.100	1.9	a	1/3	0.234	0.099	0.102	3.0
b	–	–	–	0.100	1.9	b	–	–	–	0.093	6.1

TABLE 2. Growth rate measurements and comparison with theoretical estimates for different periodic and random realizations of $f(t)$. Relative errors $Er = |\sigma_\tau - \sigma_{th}|/\sigma_{th}$ always stay small. Different realizations of the signals a and b find very similar growth rates.

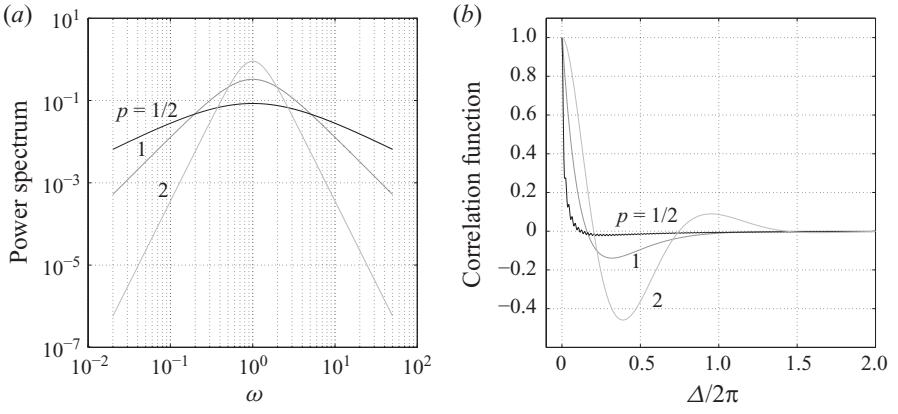

FIGURE 8. Characteristics of the random signals $f(t)$. (a) The power spectra are broadband and peak at $\omega = 1$. (b) The resulting signal is correlated over short times, illustrated here by the real part of auto-correlation function $\mathrm{Re}[\overline{f^*(t)\, f(t-\Delta)}]$.

In figure 8 we plot some features of the signals $f(t)$ for various exponents $p = 2, 1, 1/2$. Figure 8(a) shows the power spectra related to $f(t)$ for different p, clearly broadband for small p, but always peaked around $\omega = 1$ by construction. In figure 8(b), we show the real part of the auto-correlation function $\mathrm{Re}[\overline{f^*(t)\, f(t-\Delta)}]$. The signal is auto-correlated over short times, often smaller than the period 2π of the dominant wave in the spectrum.

In figure 9, we show time series for the growth of the magnetic energy. There is a clear signature of the slow exponential growth on the τ-time scale, that is independent of the realizations a or b of the phase noises. On short time scales, the signal fluctuates rather strongly compared to the previous case of periodical flows.

The slow growth rate σ_τ can be measured as before, but this measure is now subject to errors which were not present in the previous cases. Depending on the window over which the fit is performed, the growth rate σ_τ may vary over 5 %–10 %. This only reflects the fact that one cannot define a finite $\widetilde{T}$ that results in a perfect averaging process (see (A 1)) for random flows. Here we fitted over almost the entire time span.

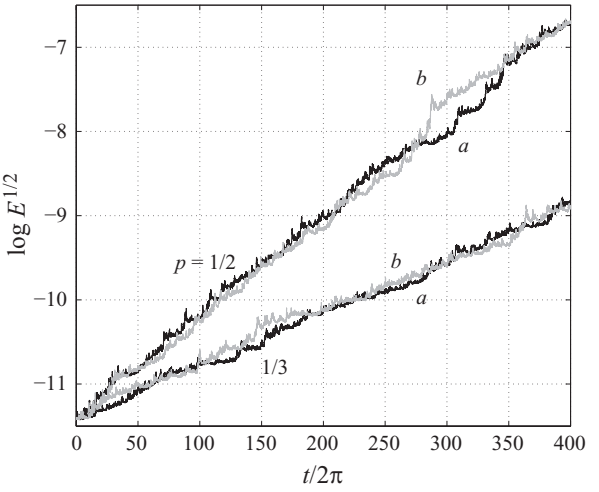

FIGURE 9. Temporal growth of energy $E = \int\int (b_x^2 + b_y^2)\,\mathrm{d}x\,\mathrm{d}y$ using two different realizations (a and b) of random signals $f(t)$ with exponents $p = 1/2$ and $1/3$.

In table 2 we compare σ_τ to the theoretical estimates $\sigma_{th} = F\,\sigma_{GO}(\mathscr{R}F)$. There is a very good agreement for all studied signals and the quantitative value of the growth rate is mostly independent of the realization of the phase noise.

3.4. *Conclusion of test*

Using our fluctuation flows $\boldsymbol{U}$, we indeed found G. O. Roberts-like dynamos. We measured an excellent quantitative agreement between (i) the direct computations and (ii) our Stokes drift model. This confirms the validity of our calculations and statements. As long as we stay close to the asymptotic limit $S \ll 1$, $Q \ll 1$ and $\mathscr{R} > 1$, we have an operational mean-field dynamo theory based on the short correlation time-approximation in the low diffusivity limit.

4. Application: simple inertial wave dynamos

Inertial waves arise in rapidly rotating flows due to the presence of the Coriolis force. They are excited in precessionally driven flows (Tilgner 2005), tidal instabilities (Kerswell 2002; Lacaze *et al.* 2006) and librational instabilities (Noir *et al.* 2009). Since the pioneering work of Moffatt (1975) who studied mean-field generation by random superpositions of inertial waves using a spatially averaged mean-field theory, much has been speculated about magnetic field generation by such flows. Numerical simulations of precessionally driven flows are starting to yield some answers (Tilgner 2005; Wu & Roberts 2008, 2009).

Inertial waves are always three-dimensional flows, so it is not excluded that even a single wave might drive a dynamo. For the time being, no numerical study has tested whether a single inertial wave can drive a kinematic dynamo. Wu & Roberts (2008) do suggest in their article that a single resonant pair of inertial waves has difficulties in driving a dynamo in a plane fluid layer.

Another typical feature of inertial waves is that they oscillate on very quick time scales (rotation period). This makes the present Stokes drift model perfectly adapted to study whether such inertial waves may drive a dynamo. We recall basic properties

and give the necessary information on the spatial structures that will allow us to apply the Stokes drift model.

4.1. *Basic properties of inertial waves*

We consider a fluid rotating around the vertical z-axis at uniform rotation speed Ω and consider perturbation flows of this base state. We take R and U as typical space scale (container size) and amplitude of these perturbations and ν as the kinematic viscosity of the fluid, we require that Rossby and Ekman numbers stay sufficiently small

$$Ro = \frac{U}{\Omega R} \ll 1, \quad E = \frac{\nu}{\Omega R^2} \ll 1. \tag{4.1}$$

In this double limit, we can find inertial waves of the form

$$\boldsymbol{U}(\boldsymbol{x}, t) = \boldsymbol{u}(\boldsymbol{r})\, \mathrm{e}^{\mathrm{i}\omega t} + \text{c.c.} \tag{4.2}$$

as solutions of the linear non-viscous perturbation problem (rotating frame)

$$i\omega \boldsymbol{u} + 2\Omega\, \hat{\boldsymbol{z}} \times \boldsymbol{u} + \nabla p = 0, \quad \nabla \cdot \boldsymbol{u} = 0. \tag{4.3}$$

A general property of such waves (Greenspan 1968) is that frequencies can only range in the interval $\omega \in [-2, 2]\Omega$. Slow waves with $\omega \ll \Omega$, will be mostly z-independent through the Taylor-Proudmann theorem and asymptote towards quasi-geostrophic Rossby waves. Whenever the flow is bounded, we need to solve (4.3) with a non-viscous boundary condition

$$\boldsymbol{u} \cdot \boldsymbol{n} = 0|_{\delta V} \tag{4.4}$$

on the boundary surface with normal $\boldsymbol{n}$. Smooth analytical solutions to these equations have only been found in particular fluid domains. We consider these cases and list some information on the spatial structure of these solutions that will be necessary to calculate the Stokes drift associated with these waves.

(*a*) Infinite space: in unbounded fluid domains, we can find plane wave solutions. Without loss of generality, we can assume a single wave to be independent of the y-coordinate. The spatial profiles that solve (4.3) are then defined as

$$\boldsymbol{u} = \frac{1}{2\sqrt{2}} \left(\omega\, \hat{\boldsymbol{x}} + 2i\, \hat{\boldsymbol{y}} - \frac{k\omega}{l}\, \hat{\boldsymbol{z}} \right) \mathrm{e}^{\mathrm{i}(kx+lz)}, \tag{4.5}$$

with k and l being, respective, horizontal and vertical wavenumbers and $\omega = \pm 2l/\sqrt{k^2 + l^2}$. The numerical prefactor assures the normalisation $|\boldsymbol{u}|^2 = 1$ everywhere in space.

(*b*) Plane fluid layer: the fluid is vertically constrained by a pair of impermeable horizontal plates, separated by a distance H that serves as length scale, $[\boldsymbol{x}] = H$. The simplest solution that fits the boundary condition is a superposition of an upward- and downward-propagating plane wave of the previous case with $l = n\pi$, $n \in \mathbb{N}_0$. More precisely, we have

$$\boldsymbol{u} = \frac{1}{2} \left(\omega \cos lz\, \hat{\boldsymbol{x}} + 2i \cos lz\, \hat{\boldsymbol{y}} - i\frac{k\omega}{l} \sin lz\, \hat{\boldsymbol{z}} \right) \mathrm{e}^{\mathrm{i}kx}, \tag{4.6}$$

with wavenumbers and frequencies k, l, ω defined as in the previous case. This profile is normalised so that $\int_0^1 |\boldsymbol{u}|^2 \mathrm{d}z = 1$.

(*c*) Cylinders, spheres and spheroids: when the waves are confined in cylindrical and spherical domains, solutions are best expressed using cylindrical coordinates (r, ϕ, z). For the purpose of the present study, we only need to remember that the

waves have the structure

$$\boldsymbol{u} = [U(r,z)\,\hat{\boldsymbol{r}} + i\,V(r,z)\,\hat{\boldsymbol{\phi}} + W(r,z)\,\hat{\boldsymbol{z}}]\,\mathrm{e}^{\mathrm{i}m\phi}, \tag{4.7}$$

with U, V, W being real functions and $m \in \mathbb{Z}$ is the azimuthal wavenumber. The confinement discretises the solutions and inertial wave dispersion relations are known since a long time (Kelvin 1880; Bryan 1889) in cylinders and spheres. In spheroidal geometry, one uses spheroidal coordinates (μ, ϕ, ν), but we still have

$$\boldsymbol{u} = [U(\mu,\nu)\hat{\boldsymbol{\mu}} + i\,V(\mu,\nu)\hat{\boldsymbol{\phi}} + W(\mu,\nu)\hat{\boldsymbol{\nu}}]\,\mathrm{e}^{\mathrm{i}m\phi}. \tag{4.8}$$

Explicit formulae and dispersion relations have been revealed by Zhang, Liao & Earnshaw (2004) through a distinct amount of analytical work.

4.2. *Simple inertial wave dynamos?*

The kinematic dynamo problem is defined in (2.5) with dimensionless numbers S and Q that may be written as

$$S = \frac{U}{\Omega R}\frac{\Omega}{\omega} = Ro\frac{\Omega}{\omega}, \quad Q = \frac{\eta}{\Omega R^2}\frac{\Omega}{\omega} = E_m\frac{\Omega}{\omega}. \tag{4.9}$$

Since both magnetic Rossby number $Ro \ll 1$ and the magnetic Ekman number $E_m \ll 1$ are generally small in a geophysical context, we can satisfy the demands of the Stokes drift model when

$$\max(Ro, E_m) \ll \frac{\omega}{\Omega}, \quad Rm = \frac{Ro}{E_m} \gg 1. \tag{4.10}$$

This is quite a weak constraint and many inertial wave flows ideally fit in our model. We now calculate the Stokes drift $\boldsymbol{V}_{st}$ associated with simple inertial wave flows in the different fluid domains considered above:

(*a*) Infinite space: $\boldsymbol{V}_{st} = \boldsymbol{0}$.

(*b*) Plane fluid layer: $\boldsymbol{V}_{st} = -\left(\dfrac{k\,\lambda^2}{2}\right)\cos(2lz)\,\hat{\boldsymbol{x}}$.

(*c*) Cylinders and spheres: $\boldsymbol{V}_{st} = -2[\,\partial_z(VW) - \partial_r(UW)]\hat{\boldsymbol{\phi}}$.

In spheroidal geometry we replace r, z by μ, ν in the last formula. The Stokes drift is absent, a one-dimensional flow or a pure circulation. If we now use these Stokes drifts in the mean-field induction equation (2.45), we find that dynamo is excluded by familiar antidynamo theorems (Bullard & Gellman 1954; Backus 1958) or (Moffatt 1978, § 6.7). Our model predicts that simple inertial waves cannot drive dynamos at leading-order.

5. Conclusion

In the present paper, we demonstrated the prominent role of the Stokes drift in dynamos driven by rapid fluctuation flows. The Stokes drift acts as a mean flow on the mean magnetic field.

We illustrated our idea in the frozen flux limit through a Lagrangian approach. We then derived an Eulerian mean-field dynamo theory which confirmed our findings and extended it to the low diffusivity regime. In particular, we showed how the effect

of Stokes drift can be deduced from the classical alpha and beta tensors in the SOCA low diffusivity limit for flows with short correlation times.

We tested our result on a series of well-chosen two-dimensional fluctuation flows that have a G. O. Roberts-like Stokes drift. The fact that Roberts-like dynamos were indeed excited and the excellent quantitative agreement between direct simulations and our model confirmed the validity of our ideas.

We finally applied our model to the question of whether single inertial waves can drive a dynamo. We computed the Stokes drift associated with these flows in the various fluid domains for which analytical profiles for the waves were available. We found that within the quite broad domain of application of our theory (4.10), these flows can never act as a dynamo at leading order.

It will be interesting to apply the present formalism to other types of flows in the geo-dynamo context. For example, can the Stokes drift associated with thermal Rossby waves drive a planetary-like dynamo?

We thank CNES for supporting this work through a postdoctoral research grant. We thank H. Latter, M. Schrinner, F. Petrelis and S. Fauve for interesting discussions about this work. We thank the three referees for their remarks which led us to considerably improve the structure, scope and readability of the paper.

Appendix A. Mean-field analysis for random flows: details

The mean-field calculation starts with deriving the classical expressions for alpha and beta tensors. Using the ansatz (2.27) and an average

$$\overline{f} = \lim_{\tilde{T}\to+\infty} \frac{1}{\tilde{T}} \int_{-\tilde{T}/2}^{\tilde{T}/2} f(t')\,\mathrm{d}t', \tag{A 1}$$

we repeat the operations (2.29)–(2.32). The fluctuation field that solves (2.32) is now found as

$$\boldsymbol{b}' = \boldsymbol{b}'(\boldsymbol{x}, t_0) + S \int_{t_0}^{t} \boldsymbol{\nabla} \times [\boldsymbol{U}(\boldsymbol{x}, t') \times \overline{\boldsymbol{b}}(\boldsymbol{x})]\,\mathrm{d}t'. \tag{A 2}$$

This solution is used to calculate the mean emf $\boldsymbol{\zeta} = S\overline{\boldsymbol{U} \times \boldsymbol{b}'}$ that takes the form (2.34) with (2.49) for alpha and beta tensors. To get to these expressions, one needs to use initial times $t_0 = -\infty$, change the integration variable into $t' = t - \Delta$ and use the property of stationarity.

To find the simplifications, we first use (2.48) in (2.49) and split the spectra in real and imaginary parts,

$$\alpha_{il} = S^2 \int_{-\infty}^{+\infty} \mathrm{d}\omega \int_{0}^{+\infty} \epsilon_{ijk} \left[\mathrm{Re}\big(\Psi^l_{jk}(\boldsymbol{x}, \omega)\big) + i\,\mathrm{Im}\big(\Psi^l_{jk}(\boldsymbol{x}, \omega)\big) \right] \mathrm{e}^{\mathrm{i}\omega\Delta}\,\mathrm{d}\Delta, \tag{A 3}$$

and similarly for the beta tensor. We then perform the integration over Δ for real and imaginary parts separately, referring to them with a suffix (R) and (I).

Writing out the definition of the real part operator, we recognise the time integration as the Fourier definition of a delta distribution $\mathscr{F}_\omega(1) = 2\pi\delta(\omega)$. Integration over ω leads to the expressions for α^{R}_{il} and β^{R}_{ilk} presented in the text. Indeed, owing to the reality of the flow

$$\Phi^*_{ij}(\boldsymbol{x}, \omega) = \Phi_{ij}(\boldsymbol{x}, -\omega), \quad \Psi^{k\,*}_{ij}(\boldsymbol{x}, \omega) = \Psi^k_{ij}(\boldsymbol{x}, -\omega) \tag{A 4}$$

and both $\Phi_{ij}(\boldsymbol{x}, 0)$ and $\Psi^k_{ij}(\boldsymbol{x}, 0)$ are real numbers.

The imaginary part of alpha is simplified using the following property:

$$\epsilon_{ijk}\left[T^l_{jk}(\boldsymbol{x},\Delta)-T^l_{jk}(\boldsymbol{x},-\Delta)\right]=\epsilon_{ijk}\,\partial_l\,R_{jk}(\boldsymbol{x},\Delta), \tag{A 5}$$

which relies solely on stationarity. Equation (A 5) translates to the spectra as

$$\epsilon_{ijk}\left[\Psi^l_{jk}(\boldsymbol{x},\omega)-\Psi^l_{jk}(\boldsymbol{x},-\omega)\right]=2i\,\epsilon_{ijk}\,\mathrm{Im}\left(\Psi^l_{jk}(\boldsymbol{x},\omega)\right)=\epsilon_{ijk}\,\partial_l\,\Phi_{ij}(\boldsymbol{x},\omega). \tag{A 6}$$

We recognise this expression in the integrandum of the α^{I}_{il} part. The time integral over Δ is the Fourier transform of the Heaviside function, $\mathscr{F}_\omega(1-H(\Delta))=-1/i\,\omega+\pi\,\delta(\omega)$. With $\epsilon_{ijk}\,\Phi_{jk}(\boldsymbol{x},0)=0$ for real flows, one then finds

$$\alpha^{\mathrm{I}}_{il}=\partial_l\left[S^2\int_0^{+\infty}\mathrm{Im}\left(\frac{\epsilon_{ikj}\,\Phi_{jk}(\boldsymbol{x},\omega)}{\omega}\right)\mathrm{d}\omega\right]=\partial_l\,\xi_i. \tag{A 7}$$

The α^{I}-term has the exact same structure as in the single wave case and defines the $\boldsymbol{\xi}$-field. The β^{I}-term is calculated using the same Fourier transform

$$\beta^{\mathrm{I}}_{ilk}=S^2\int_0^{+\infty}2\,\mathrm{Im}\left(\frac{\epsilon_{ijk}\,\Phi_{jl}(\boldsymbol{x},\omega)}{\omega}\right)\mathrm{d}\omega. \tag{A 8}$$

The components of this tensor with all different indices, $i\neq l\neq k$, disappear because the imaginary part of the autocorrelation spectra identically disappears for real flows,

$$\mathrm{Im}(\Phi_{ii}(\boldsymbol{x},\omega))=0,\quad i=1,2,3. \tag{A 9}$$

Exceptionally, the double index i does not represent a sum in this formula. Components with $i=k$ disappear because of the Levi-Civita tensor. The remaining components take the same form as in the single wave case (see (2.39)) and α^{I} and β^{I} terms similarly recombine to the Stokes drift. The total mean emf finally takes the form (2.50) with supplementary terms from the zero-frequency spectra.

Appendix B. Compressible flows

It is possible to account for the effects of compressibility $\boldsymbol{\nabla}\cdot\boldsymbol{U}\neq 0$. We illustrate this here in the simple wave case. The first time where we meet the effects of compressibility is in the evaluation of $\boldsymbol{b}'$

$$\boldsymbol{b}'=\boldsymbol{b}'(\boldsymbol{x},t_0)+S\left[-i\left(\overline{\boldsymbol{b}}\cdot\boldsymbol{\nabla}\boldsymbol{u}-\boldsymbol{u}\cdot\boldsymbol{\nabla}\overline{\boldsymbol{b}}-\overline{\boldsymbol{b}}\,(\boldsymbol{\nabla}\cdot\boldsymbol{u})\right)\mathrm{e}^{\mathrm{i}t}+\mathrm{c.c.}\right]. \tag{B 1}$$

The fluctuation field receives a supplementary term that involves the divergence of the spatial profiles $\boldsymbol{u}$ of the waves. If we calculate the emf $\boldsymbol{\zeta}$, we find alpha and beta tensors as before (see (2.35)) and a supplementary contribution that has the structure of a 'pumping' term

$$\zeta_i=\alpha_{il}\,\overline{b}_l+\beta_{ilk}\,\partial_l\,\overline{b}_k+\left(\mathscr{U}\times\overline{\boldsymbol{b}}\right)_i, \tag{B 2}$$

with

$$\mathscr{U}=-2\,S^2\,\mathrm{Im}\left[\boldsymbol{u}^*(\boldsymbol{\nabla}\cdot\boldsymbol{u})\right]. \tag{B 3}$$

After the same simplifications as specified in the text, the emf takes the form

$$\boldsymbol{\zeta}=\left(\boldsymbol{\nabla}\times\boldsymbol{\xi}+\mathscr{U}\right)\times\overline{\boldsymbol{b}}+\boldsymbol{\nabla}\left(\boldsymbol{\xi}\cdot\overline{\boldsymbol{b}}\right), \tag{B 4}$$

with $\boldsymbol{\xi}$ still defined as before (see (2.38)). Again the only mean-field effect seems to be that of a total flow that initially seems to be different from the Stokes drift in the compressible case. However, looking in more detail we find

$$(\boldsymbol{\nabla}\times\boldsymbol{\xi}+\mathscr{U})_i=2\,S^2\,\mathrm{Im}\left[\partial_j\left(u_i^*u_j\right)-u_i^*\,\partial_j\,u_j\right]=2\,\mathrm{Im}\left(u_j\,\partial_j\,u_i^*\right)=(\boldsymbol{V}_{st})_i, \tag{B 5}$$

which is identical to the previous expression in the incompressible case. All final formulae for the mean-field evolution (2.45) and (2.53) for incompressible flows can also be used for compressible flows.

Appendix C. Small mean flow

Flows that have a small mean part $\overline{\boldsymbol{U}} = \overline{\boldsymbol{U}} = S^2\overline{\widetilde{\boldsymbol{U}}} = O(S^2)$ can be included without any problem in the model as such small mean flow cannot modify the fluctuation field at order $O(S)$. It however needs to be considered in the mean-field equation. We replace (2.45) and (2.53) by

$$\sigma_\tau \overline{\boldsymbol{b}} = \boldsymbol{\nabla} \times [(\overline{\widetilde{\boldsymbol{U}}} + \boldsymbol{V}_{st}) \times \overline{\boldsymbol{b}}] + \mathscr{R}^{-1} \Delta \overline{\boldsymbol{b}} + \cdots \tag{C 1}$$

to take this mean flow into account. It will be necessary to consider this small extension whenever one wishes to discuss kinematic dynamo action by forced hydrodynamical waves. Next to the Stokes drift, the 'streaming'-flow induced by nonlinear interactions of pairs of waves can have the same magnitude as the Stokes drift term $O(S^2)$. See, for example, Falkovich (2009) for a recent discussion on this issue in the context of mixing by gravity waves.

REFERENCES

Aldridge, K. D. & Toomre, A. 1969 Axisymmetric inertial oscillations of a fluid in a rotating spherical container. *J. Fluid Mech.* **37**, 307–323.

Backus, G. E. 1958 A class of self-sustaining dissipative spherical dynamos. *Ann. Phys.* **4**, 372–447.

Braginsky, S. I. 1964 Self excitation of a magnetic field during the motion of a highly conducting fluid. *Sov. Phys. JETP* **20**, 726–735.

Brandenburg, A. 2009 Advances in theory and simulation of large-scale dynamos. *Space Sci. Rev.* **1–4**, 87–104.

Bryan, G. H. 1889 The waves on a rotating liquid spheroid of finite ellipticity. *Phil. Trans. R. Soc. Lond.* **A180**, 187–219.

Bullard, E. & Gellman, H. 1954 Homogeneous dynamos and terrestrial magnetism. *R. Soc. Lond. Phil. Trans. Ser. A* **247**, 213–278.

Busse, F. H. 2002 Convective flows in rapidly rotating sphere and their dynamo action. *Phys. Fluids* **14**, 1301.

Childress, S. & Gilbert, A. D. 1995 *Stretch, Twist, Fold: The Fast Dynamo*. Springer.

Christensen, U. R. 2008 Earth science: a sheet-metal geodynamo. *Nature* **454**, 1058–1059.

Courvoisier, A., Hughes, D. W. & Tobias, S. M. 2006 Alpha effect in a family of chaotic flows. *Phys. Rev. Lett.* **96** (3), 034503.

Falkovich, G. 2009 Could waves mix the ocean. *J. Fluid Mech.* **638**, 1–4.

Glatzmaier, G. A. & Roberts, P. H. 1995 A three-dimensional self-consistent computer simulation of a geomagnetic field reversal. *Nature* **377**, 203–209.

Greenspan, H. P. 1968 *The Theory of Rotating Fluids*. Cambridge University Press.

Kelvin, Lord 1880 Vibrations of a columnar vortex. *Phil. Mag.* **10**, 155–168.

Kerswell, R. R. 2002 Elliptical instability. *Annu. Rev. Fluid Mech.* **34**, 83–113.

Krause, F. & Rädler, K.-H. 1980 *Mean-Field Magnetohydrodynamics and Dynamo*. Berlin and Pergamon Press.

Lacaze, L., Herreman, W., Le Bars, M., Le Dizès, S. & Le Gal, P. 2006 Magnetic field induced by elliptical instability in a rotating spheroid. *Geophys. Astrophys. Fluid Dyn.* **100**, 299–317.

Malkus, W. V. R. 1968 Precession of the Earth as the cause of geomagnetism. *Science* **160** (3825), 259–264.

Moffatt, H. K. 1975 Dynamo action associated with random inertial waves in a rotating conducting fluid. *J. Fluid Mech.* **44**, 705–719.

Moffatt, H. K. 1978 *Magnetic Field Generation in Electrically Conducting Fluids*. Cambridge University Press.

Molchanov, S. A., Ruzmaikin, A. A. & Sokolov, D. D. 1985 Kinematic dynamo in random flow. *Sov. Phys. Uspekhi* **28**, 307–327.

Noir, J., Hemmerlin, F., Wicht, J., Baca, S. M. & Aurnou, J. M. 2009 An experimental and numerical study of librationally driven flow in planetary cores and subsurface oceans. *Phys. Earth Planet. Inter.* **173** (1–2), 141–152.

Plunian, F. & Rädler, K.-H. 2002 Harmonic and subharmonic solutions of the roberts dynamo problem. application to the karlsruhe experiment. *Magnetohydrodynamics* **38** (1–2), 92–103.

Rädler, K.-H. & Brandenburg, A. 2009 Mean-field effects in the galloway-proctor flow. *Mon. Not. R. Astron. Soc.* **393** (1), 113–125.

Rädler, K.-H., Rheinhardt, M., Apstein, E. & Fuchs, H. 2002 On the mean-field theory of the karlsruhe dynamo experiment. Part I. kinematic theory. *Magnetohydrodynamics* **38** (1–2), 39–69.

Roberts, G. O. 1972 Dynamo action of fluid motions with two-dimensional periodicity. *Phil. Trans. R. Soc. Lond.* **A271**, 411–454.

Schrinner, M., Rädler, K. H., Schmitt, D., Rheinhardt, M. & Christensen, U. 2007 Mean-field concept and direct numerical simulations of rotating magnetoconvection and the geodynamo. *Geophys. Astrophys. Fluid Dyn.* **101**, 81–116.

Soward, A. M. 1987 Fast dynamo action in a steady flow. *J. Fluid Mech.* **180** (1), 267–295.

Stieglitz, R. & Muller, U. 2001 Experimental demonstration of a homogeneous two-scale dynamo. *Phys. Fluids* **13**, 561–564.

Stokes, G. G. 1847 On the theory of oscillatory waves. *Trans. Camb. Phil. Soc.* **8**, 441–455.

Sur, S., Brandenburg, A. & Subramanian, K. 2008 Kinematic alpha effect in isotropic turbulence simulations. *Mon. Not. R. Astron. Soc.* **385**, L15–L19.

Tilgner, A. 2005 Precession driven dynamos. *Phys. Fluids* **17**, 034104.

Wu, C. C. & Roberts, P. H. 2008 A precessionally-driven dynamo in a plane layer. *Geophys. Astrophys. Fluid Dyn.* **102**, 1–19.

Wu, C. C. & Roberts, P. H. 2009 On a dynamo driven by topographic precession. *Geophys. Astrophys. Fluid Dyn.* **103** (6), 467–501.

Zhang, K., Liao, X. & Earnshaw, P. 2004 On inertial waves and oscillations in a rapidly rotating spheroid. *J. Fluid Mech.* **504**, 1–40.